Available online at www.sciencedirect.com
SCIENCE DIRECT®
Organic Electronics 4 (2003) 209–218
Organic Electronics
www.elsevier.com/locate/orgel

Interface instabilities in polymer light emitting diodes due to annealing

F.J.J. Janssen [a], J.M. Sturm [a], A.W. Denier van der Gon [a], L.J. van IJzendoorn [a,*], M. Kemerink [b], H.F.M. Schoo [c], M.J.A. de Voigt [a], H.H. Brongersma [a]

[a] Department of Applied Physics, Eindhoven University of Technology, P.O. Box 513, 5600 MB Eindhoven, The Netherlands
[b] COBRA Inter-University Research Institute, P.O. Box 513, 5600 MB Eindhoven, The Netherlands
[c] TNO Institute of Industrial Technology, P.O. Box 6235, 5600 HE Eindhoven, The Netherlands

Received 19 November 2002; received in revised form 15 May 2003; accepted 21 June 2003

Abstract

In polymer light emitting diodes (PLEDS) with an (ITO/PPV/Ca) structure we observed a significant reduction of both the current and the light output at constant voltage after heat treatment for only 30 min at 65 °C. Electroluminescence spectroscopy experiments showed that the shape as well as the amplitude of the spectra were changed.

The reduction of current and light output was investigated by measuring *I–V* and *E–V* (current–voltage and brightness–voltage) characteristics of PLEDs, *I–V* characteristics of single carrier devices, and by performing low energy ion scattering and X-ray photoelectron spectroscopy experiments on the Ca/PPV interface.

It was concluded that the current and light output reduction could be ascribed to the degradation of the Ca/PPV and the ITO/PPV interfaces. The degradation of the ITO/PPV interface resulted in a reduction of the zero field hole mobility and a small increase of the field dependence of the mobility. The degradation of the Ca/PPV interface, probably by diffusion of calcium into the PPV, resulted in carrier traps and quenching sites, which influenced the field dependent electron mobility.

PACS: 85.60 Jb; 81.05 Lg; 81.40 Ef
Keywords: Conjugated polymers; Light emitting devices; Annealing; Interface; Stability

1. Introduction

Polymer light emitting diodes (PLEDs) are considered promising candidates for full colour, cheap, flexible displays, which are easy to process [1,2]. The colour of emission of the device can be tuned over the full visible spectrum by tuning the bandgap of the polymer [3]. The simplest PLEDs consist of an emitting polymer layer (often derivatives of poly-*p*-phenylene vinylene (PPV)), which is sandwiched between an anode (usually ITO) and a cathode (e.g. Ca, Al). Often the glass/ITO/PPV structure is heated [4] before application of the cathode in order to remove oxygen, water and

* Corresponding author. Tel.: +31-40-2474341; fax: +31-40-2438060.
E-mail address: l.j.van.ijzendoorn@tue.nl (L.J. van IJzendoorn).

1566-1199/$ - see front matter © 2003 Elsevier B.V. All rights reserved.
doi:10.1016/S1566-1199(03)00017-X

residual solvent from the PPV. The device is also exposed to heat radiation of the evaporator, when a protective Al layer is applied. Furthermore, commercial applications require a certain stability over a specific temperature range. Lee and Park [4] showed that annealing of PLEDs with Al cathodes has a positive effect on the power efficiency and the light output, which was attributed to enhanced interface adhesion between Al and PPV by improved chemical interaction.

In existing studies on metal/PPV interfaces [5,6] the chemical interaction between metal and PPV was considered. For calcium it was found that it ionises and dopes the PPV thereby creating states in the band gap, but this was not related directly to PLED operation. Effects of (minor) heat treatment were not considered, and therefore also not the influence of the change of the interfaces on the PLED performance. We report here on the effects of heat treatment on PLEDs with calcium cathodes, as studied by electrical characterisation of PLEDs as well as hole dominated (ITO/PPV/Au and Au/PPV/Au) and electron dominated (TiN/PPV/Ca) devices. Furthermore, with low energy ion scattering (LEIS) and X-ray photoelectron spectroscopy (XPS) the Ca/PPV interface stability was studied.

2. Experimental

2.1. Preparation of PLEDs

Substrates of glass covered with ITO (100 nm ITO, Merck) were cleaned successively with acetone (Uvasol, Merck) and 2-propanol (Uvasol, Merck), applied each for 10 min in an ultrasonic bath. Next, a UV ozone treatment was applied for 20 min. Subsequently, the UV-ozone chamber was pumped down and flushed with nitrogen, and the samples were transferred without getting into contact with air to a glove box (O_2 and $H_2O < 1$ ppm), where an OC_1C_{10} PPV (poly(dialkoxy-*p*-phenylene vinylene)) layer was spin-coated directly onto the ITO from an 0.5–0.7 wt% PPV solution in toluene. Then, the specimens were transferred from the glove box into a transfer chamber without contact to air. Next, the transfer chamber was pumped down to 5×10^{-7} mbar in about 20 min and the samples were transported to the evaporation chamber. Here an 80 nm thick calcium cathode was evaporated from an effusion cell, at a deposition rate of 0.3 nm/s. The pressure during the evaporation was $\sim1\times10^{-7}$ mbar, the residual gas consisted almost entirely of hydrogen (the partial oxygen and water pressures were lower than 10^{-9} mbar, as measured with a mass spectrometer). Electrical and optical characteristics were measured in the evaporation chamber.

Heat treatment was performed in the evaporation chamber with an infrared lamp; the temperature was measured with NTC thermistors (accuracy ±3 °C), which were in contact with the glass substrate of the PLEDs. After the heat treatment the samples were cooled down before electrical and optical characteristics were measured.

Hole and electron single carrier devices were prepared by variation of cathode and anode materials. Hole single carrier devices consisted of glass/ITO/PPV/Au and glass/Au/PPV/Au structures. Glass/TiN/Ca/PPV electron single carrier devices were made according to Bozano et al. [7]. For both glass/Au and glass/TiN the same cleaning procedure as for glass/ITO was performed except for the UV ozone treatment, which was omitted to avoid destruction of the TiN or the Au layer.

Differences in morphology and/or roughness of the PPV surface will influence the PPV/metal interface formation, and therefore the electronic properties of the PLED. Tapping mode atomic force microscopy (AFM) measurements were performed on glass/Au/PPV, glass/ITO/PPV and glass/TiN/PPV samples, to study the effect of the anode on the surface of the PPV layer. It was concluded that within the experimental accuracy the surface roughness was equal for all three samples (RMS = 0.7 nm on 500×500 nm images). Furthermore no difference in structure or ordering were observed from the AFM images.

2.2. Low energy ion scattering

LEIS [8] is a technique that can probe the outermost atomic layer of a sample. A beam of low energy noble gas ions is directed onto a sample

and the energy spectrum of the (back)scattered ions is measured. The energy of a scattered ion depends on the atom the interaction took place with, and therefore the energy spectrum of scattered ions reflects the atomic mass distribution of the sample surface. The incoming ions that are not scattered by atoms in the outermost layer, penetrate the sample and are neutralised. This method is surface-sensitive because the analyser of the LEIS set-up accepts only ions.

However, in the case of calcium on PPV the situation becomes more complex because the reionisation probability of calcium is very high [9]. As a result, He ions that are neutralised upon penetration of the sample, can be reionised upon emerging from the sample. Thus not only calcium at the surface, but also calcium which resides below the surface contributes significantly to the calcium peak, resulting in a broadening of the peak at the low energy side. This will be further discussed in Section 3.4.

Glass/ITO/PPV samples were prepared in the glove box as described above and transferred under nitrogen atmosphere to the LEIS/XPS set-up. In a separate compartment of the LEIS/XPS set-up calcium was evaporated and heat treatment was performed. The pressure during evaporation calcium was 10^{-7} mbar. The LEIS experiments were carried out with 3 keV $^3He^+$ ions.

3. Results

3.1. PLEDs

Fig. 1 shows the average relative current and light output at 6 V after heat treatment at various annealing temperatures of PLEDs consisting of glass/ITO/PPV/Ca. For each temperature at least 12 devices were prepared and measured in at least two batches, the deviations between devices were smaller than 5%. In Fig. 2 the *I–V* (current–voltage) and *E–V* (light output–voltage) characteristics for a PLED, before and after heat treatment for 30 min at 65 °C, are plotted. It can be seen from both Figs. 1 and 2 that heat treatment leads to a strong current and light output reduction. Furthermore, it is obvious that the current and light output reduction is correlated to the annealing temperature. It should be noted that without heat treatment a reduction in the current and the light output of only a few percent was observed after leaving the PLED for 100 min (the time needed to perform the heat treatment and the cooling down) in vacuum.

In Fig. 1 the reduction of current and light output after evaporation of 50 nm of aluminium on top of the calcium is also shown. The temperature of the PLEDs increased during evaporation because of the radiation of the aluminium

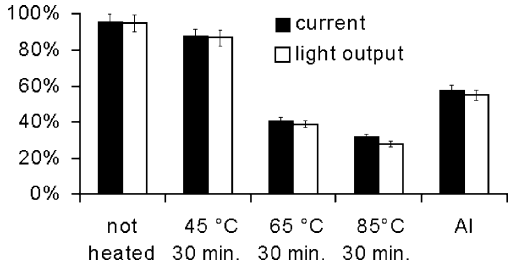

Fig. 1. Averaged current and light output at 6 V of PLEDs (ITO/PPV/Ca) after different heat treatments. The bars are normalised to the current and the light output before the heat treatment. The first two bars are measured at untreated PLEDs 100 min after the first measurement, which is comparable to the time needed for the heat treatment and the cooling down process. The 'Al' bar is measured at a device (ITO/PPV/Ca) on which 50 nm of Al is deposited instead of performing an annealing procedure.

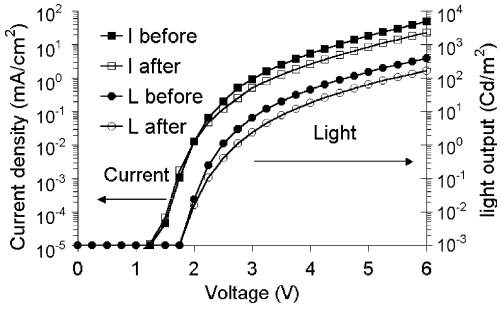

Fig. 2. Electrical (I) and optical (L) characteristics of a representative PLED with Ca cathode before and after heat treatment. Heat treatment at 65 °C for 30 min was performed in high vacuum ($\sim 10^{-9}$ mbar). The temperature during measurement was 38 °C both before and after heat treatment. The lines connecting the points are drawn to guide the eye. For clarity minimal currents are set to 10^{-5} mA/cm^2, which equals the detection limit of our set-up.

evaporator. Temperature measurements on the backside of the PLED indicated temperatures of 48 °C immediately after the evaporation of the aluminium. It was verified that the electrical characterisation itself does not lead to a degradation of the PLED performance. This was concluded from a comparison of the *I–V* and *E–V* characteristics measured after the heat treatment of PLEDs characterised and not characterised prior to the heat treatment.

Subsequently, experiments were performed to find the origins of the current and light output reductions. Therefore, heat treatments at 65 °C for 30 min were applied at different stages in the production process. First, samples were annealed before the calcium cathode was applied, see Table 1. Heat treatment before application of the cathode led to a smaller reduction in the current and light output than heat treatment after application of the cathode. Heat treatment both before and after application of the cathode resulted in the same current and light output reduction as heat treatment after application of the cathode. Furthermore, Table 1 indicates that the voltage at which the maximum power efficiency (Cd/A) occurs increased after heat treatment, and that the increase was largest if heat treatment was applied with the cathode present.

Next, the electroluminesence spectra of PLEDs were measured before and after heat treatment (Fig. 3). It can be seen that apart from an overall decrease in intensity, the shape of the spectrum changed. Ruhstaller et al. [10] stated that in the emission spectrum of conjugated polymers typically two vibronic features can be observed, which can be assigned to the (0–0) and the (0–1) vibronic transitions. The shape of the spectrum and the separation of the peaks are comparable to the values in [11,12]. Therefore, we assigned the two peaks of the shortest wavelengths to the 0–0 and the 0–1 vibronic transitions. The emission at longer wavelengths (>620 nm) results from ag-

Table 1
Current density, light output and efficiency of ITO/PPV/Ca PLEDs at 6 V normalised to the values of an untreated device. Heat treatment is conducted for 30 min at 65 °C. The absolute values of an untreated device were ~50 mA/cm^2 for the current and 400 Cd/m^2 for the light output; all devices were ~120 nm thick

	Current	Light output	Efficiency	Voltage of max efficiency (V)
Untreated	1	1	1	4.1 ± 0.3
Heat after Ca deposition	0.42 ± 0.05	0.38 ± 0.05	0.9 ± 0.1	5.8
Heat before Ca deposition	0.71	0.64	0.9	4.5
Heat before and after Ca deposition	0.46	0.40	0.9	5.8

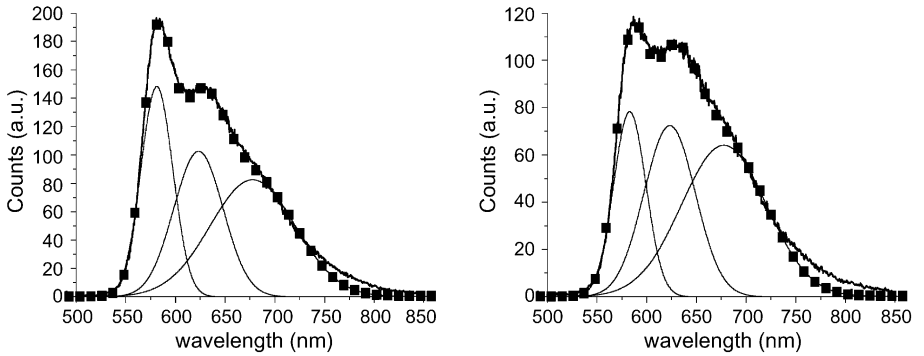

Fig. 3. Electroluminescence spectra of ITO/PPV/Ca PLEDs before (left) and after (right) heat treatment for 30 min at 65 °C. The spectrum is decomposed into three Gaussian curves for which the same position and widths are used for both curves. The dotted curves are the sum of the three Gaussian curves.

Table 2
Areas of the Gaussian peaks as obtained by fitting (Fig. 3). In the second and the fourth columns the areas are normalised to the second peak

	Area peak 1	Area peak 2	Area peak 3
Before (a.u.)	$(6.0 \pm 0.2) \times 10^3$	6.4×10^3	8.9×10^3
Relative	0.94 ± 0.04	1	1.39
After (a.u.)	$(3.2 \pm 0.2) \times 10^3$	4.7×10^3	6.9×10^3
Relative	0.68 ± 0.04	1	1.47

gregate emission [13,14]. To obtain an indication of the change in the ratios of the peak areas resulting from heat treatment, the spectra were fitted by three Gaussian peaks at fixed positions and with fixed widths [15]. In Table 2 the ratios of the peaks areas are given. Apparently, the spectral changes after heating can be attributed to a decrease of the first vibronic transition (0–0). Finally, the electroluminesence spectrum of the devices heated before calcium deposition was measured. Again, an overall decrease in intensity compared with an untreated device was observed, but the shape of the curve was not changed.

3.2. Hole only, single carrier devices

In the previous paragraph it was shown that heat treatment of PLEDs leads to a reduction of the current and the light output. In order to find the mechanism that causes the current reduction, single carrier devices were prepared by changing the electrode materials of the PLED. First, results are shown of devices for which the calcium cathode was replaced by a gold cathode. The high work function of gold blocks the injection of electrons and therefore these devices can be considered as hole only, single carrier devices. Only 20 nm of gold was used to maintain a low temperature of the device during evaporation (the deposition rate was 8–10 nm per minute). After evaporation of the cathode a heat treatment for 30 min at 65 °C was performed, the results are shown in Table 3. The reproducibility of these devices was comparable with the reproducibility of normal PLEDs.

Again, a reduction in the current density was found after heat treatment. Remarkably, the reduction in current of these devices was equal for heat treatment before and after application of the Au cathode. To get a better understanding, device modelling was performed on the ITO/PPV/Au devices, see Fig. 4. The model we used is based on the work presented in [16,17] and includes charge injection via tunnelling, thermo-ionic emission and interface recombination, transport and space charge effects. It should be emphasised that effects of interface and surface roughness, which would result in an inhomogeneous field distribution, is not incorporated. Effects of diffuse interfaces are also not taken into account. From literature [17] the following parameters were taken: an activation energy $\Delta = 0.48$ eV and a relative dielectric constant $\varepsilon_r = 3$. The following parameters were obtained from modelling untreated devices; a zero field hole mobility $\mu_0 = 4.8 \pm 0.2 \times 10^{-11}$ m^2/V s, a field dependence parameter γ of the mobility of $\gamma = 4.2 \pm 0.3 \times 10^{-4}$ (m/V)$^{1/2}$, and a hole injection barrier of 0.2 eV. The zero field mobility represents the field independent mobility for the film as prepared through spin coating. For differently prepared films with a different structural order, other values will result. This difference however cannot be distinguished from differences occurring by changes of the polymer by for instance oxidation. Modelling of the heat treated devices showed (Fig. 4) a decrease of the zero field hole mobility to

Table 3
Currents through devices with different cathode materials measured at 6 V before and after heat treatments for 30 min at 65 °C, normalised to the values of an untreated device. "Before" and "After" indicated if the device is heated before or after evaporation of the cathode

	Untreated absolute (mA/cm^2)	Before/Unt.	After/Unt.	Before and after/Unt.
ITO/PPV(180 nm)/Au	2.5	0.78 ± 0.05	0.82	0.78
Au/PPV(180 nm)/Au	2.7	1.03 ± 0.05	0.97	0.96
TiN/PPV(120 nm)/Ca	0.48	1.0 ± 0.1	0.4	0.4
Au/PPV(120 nm)/Ca	48.3	1.0 ± 0.1	0.61	–

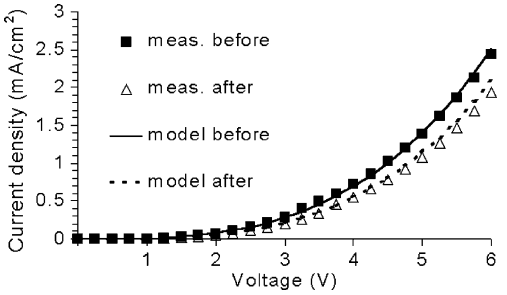

Fig. 4. Current as a function of voltage for an ITO/PPV(180 nm)/Au device before and after heat treatment for 30 min at 65 °C. The curves are derived from modelling.

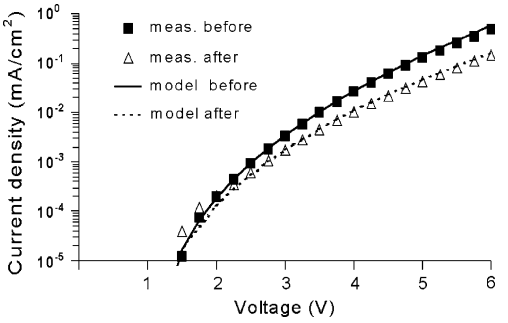

Fig. 5. Current densities as a function of voltage for a TiN/PPV(120 nm)/Ca device before and after heat treatment for 30 min at 65 °C. The curves are derived from model calculations. For clarity the minimal current is set to 10^{-5} mA/cm^2, which equals the detection limit of our set-up.

$\mu_0 = 3.4 \pm 0.2 \times 10^{-11}$ m^2/V s and an increase of the field dependence parameter of the mobility to $\gamma = 4.7 \pm 0.3 \times 10^{-4}$ (m/V)$^{1/2}$, while the hole injection barrier remained unchanged.

To separate the effects of degradation of the ITO/PPV interface and degradation of the PPV itself, devices with a gold anode and a gold cathode were prepared (Au/PPV/Au). The work function of gold is relatively high, therefore these devices are hole only, single carrier devices. The currents through untreated Au/PPV/Au devices are comparable to the currents through ITO/PPV/Au devices, so ITO and Au anodes behave more or less the same.

From Table 3 it can be seen that for the Au/PPV/Au devices no significant current reduction is found after heat treatment. Apparently the reduction of the zero field hole mobility and the increase of the field dependence of the mobility was induced by the ITO anode.

Finally, the ITO anode was replaced by gold in a PLED (Au/PPV/Ca) to see if these devices also suffer from current reduction after heat treatment. It was found that the current and light output was reduced to $61 \pm 5\%$, thus the reduction was less than in PLEDs with ITO anodes ($42 \pm 5\%$) (Table 3). Gold anodes are not suitable for PLEDs anyway, because of the relatively high reflectance of the gold.

3.3. Electron only, single carrier devices

Here we show results of measurements on devices for which the ITO anode was replaced by TiN, which is a hole blocking contact [7]. The TiN/PPV/Ca devices did not show light output in the used voltage range (0–6 V), so we concluded that the devices were electron only, single carriers. From Table 3 it can be seen that these devices only suffered from reduced currents when heat treatment was performed after application of the calcium cathodes.

Modelling of untreated devices (see Fig. 5) resulted in the following parameters: an electron injection barrier of 0.43 eV, an electron field-independent mobility $\mu_0 = 5.3 \times 10^{-13}$ m^2/V s, a field dependence parameter of the mobility of $\gamma = 8 \times 10^{-4}$ (m/v)$^{1/2}$. From literature [17] the following parameters were taken: an activation energy $\Delta = 0.48$ eV and a dielectric constant $\varepsilon_r = 3$. Devices were characterised and modelled at 40 °C. At high electric fields (>2.5×10^3 V/m) the modelled curves are in good agreement with the measurements; the difference in the current at high fields before and after heating, can be modelled by changing the field dependence of the electron mobility from $\gamma = 8 \pm 1 \times 10^{-4}$ (V/m)$^{1/2}$ to $\gamma = 4 \pm 1 \times 10^{-4}$ (V/m)$^{1/2}$.

3.4. Low energy ion scattering and X-ray photoelectron spectroscopy

A more detailed understanding into the Ca/PPV interface formation and stability was obtained with LEIS and XPS. We deposited an amount of

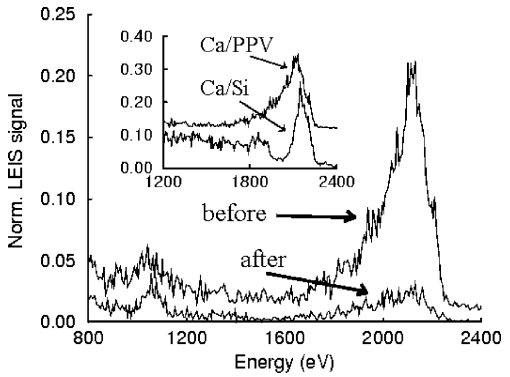

Fig. 6. LEIS spectrum of a Ca/PPV surface before and after heat treatment for 30 min at 65 °C. The surface of PPV is only covered by ~20% with calcium. The curve before heat treatment has an offset of 0.01. All spectra are normalised on the height of the calcium peak from a measurement on a sample totally covered with calcium. The inset shows a comparison between a sample with 20% surface coverage Ca on PPV (offset by 0.12) an a sample with 20% surface coverage of Ca on Si.

calcium that covered about 20–40% of the PPV surface in order to study the Ca/PPV interface with LEIS. The amount of calcium covering the PPV was quantified by comparison of the LEIS signal of the Ca on the PPV to the LEIS signal of a sample fully covered with calcium.

Fig. 6 shows the LEIS spectra of the sample before and after heat treatment. In Table 4 the LEIS peak heights and the XPS peak area ratios before and after heating are shown. It can be seen from the LEIS spectra that the calcium disappears from the surface. The calcium peak in the LEIS spectrum (before heat treatment) is broadened at the low energy site. This indicates that the interface is not sharp. The peak broadening results from He ions, which penetrate the sample and neutralise, subsequently scatter at calcium atoms below the PPV surface, and then re-ionise at the surface. The inset in Fig. 6 shows the comparison between a sample with 20% surface coverage Ca on PPV (offset 0.12) and one with 20% surface coverage on Si. On the Si sample, all Ca atoms remain on the surface, and the Ca peak thus corresponds to the peak shape of the outermost atomic layer. The Ca signal at energies below the Ca/Si peak originates from Ca in deeper layers.

Table 4
The relative peak heights before and after heating are shown as measured with LEIS and XPS. Results are normalised to the peak heights (LEIS) and the peak area (XPS) of the measurement before heat treatment. For LEIS the height of the Ca peak is taken while for the peak area of Ca in XPS is derived from the Ca to C ratio

	Before heat treatment	After heat treatment
LEIS	1	0.15
XPS	1	0.57

The decrease of the calcium peak in the LEIS spectrum should result in an increase of the carbon peak. The statistics of the carbon peak are poor because the sensitivity of LEIS for C is much lower than for Ca. By carefully subtracting the background an increase of the carbon peak area of $15 \pm 5\%$ after heat treatment is found. This is in reasonable agreement with the expected increase of 20% as estimated from the fraction of the surface covered by Ca before heating.

In the XPS signal a significant reduction in the Ca to C peak ratio was observed. To get an indication of the average depth of the calcium in the PPV we calculated how deep the calcium has to diffuse into the PPV to obtain an equal decrease in the XPS signal. We found that this signal reduction can be reached by assuming all the evaporated calcium diffused to a depth of ~3.5 nm (this is of course not a realistic model for the calcium distribution after diffusion, but only gives an idea of the extent of the diffusion). The binding energy of the Ca $2p_{3/2}$ peak had not changed after heat treatment and was found to be 346.3 ± 0.3 eV (with the hydrocarbon C 1s peak as reference at 285.0 eV). As pointed out in [18] there is not much doubt that the Ca is in a 2+ state, as measured from the Ca $2p_{3/2}$ peak shift, but it is difficult to distinguish between Ca^{2+} and an oxidised compound. However, it can be concluded that the chemical state of the Ca does not change by the heat treatment. The ratio of oxygen to carbon measured with XPS before and after heat treatment is within the experimental uncertainty equal to that of PPV. Furthermore the O 1s peak position was unchanged after heat treatment compared to the situation before heat treatment, while we observed that oxidation of the Ca/PPV interface led to a

shift of the oxygen peak of 1.2 ± 0.3 eV to lower energies and a significant increase of the oxygen to carbon ratio. In the LEIS spectrum no clear oxygen peak was visible before and after annealing. In the case calcium was oxidised by evaporation of the calcium in an oxygen ambient atmosphere (partial oxygen pressure of 10^{-6} mbar) a small oxygen peak was visible in the LEIS spectrum. We conclude from both LEIS and XPS that before and after the heat treatment the calcium was not oxidised.

4. Discussion

4.1. ITO/PPV interface

Current reduction after heat treatment in hole only, single carrier devices was only found in the ITO/PPV/Au structure and not in the Au/PPV/Au structure. From this we concluded that ITO was the cause of the current reduction in the ITO/PPV/Au hole single carrier devices. From the Au/PPV/Au structure it was concluded that the effect of the heat treatment on the PPV itself was negligible, at least concerning the hole current. It can be expected that the reduction of the hole mobility as found from the simulations, was caused by the diffusion of oxygen [19] from the ITO into the PPV.

To confirm this, glass/ITO substrates were heated for 30 min at 65 °C and studied with LEIS and XPS. In the LEIS spectra it was observed that the signal of oxygen decreased upon heat treatment. From XPS measurements, a lower O/In ratio was found after heat treatment, whereas the binding energies of In, Sn and O remained unchanged. Thus both XPS and LEIS indicate that oxygen leaves the ITO upon heating, in agreement with the hypothesis that oxygen diffusion into the PPV causes the reduced hole mobility. In [20] we showed that the presence of oxygen in PPV reduces the current through a PLED. The presence of oxygen apparently leads to higher hopping barriers in the PPV and, therefore, to a lower value of the zero field mobility and a higher value of the field dependence of the mobility [21]. The presence of oxygen might cause extra levels in the band gap by van der Waals interaction with the PPV, these extra levels act as hole traps.

Heat treatment of ITO/PPV/Au devices before evaporation of the gold cathode also led to reduced currents which indicates that once oxygen diffuses into the PPV it will remain in the film. In devices with Ca cathodes, LEIS and XPS experiments did not show increased concentrations of oxygen at the PPV/Ca interface, which indicates that the oxygen does not reach the cathode. Furthermore, additional oxygen at the calcium interface would lead to a reduced efficiency of the PLED [22], which we also do not observe. Apparently the oxygen is not, or only in very small amounts, reaching the calcium cathode and therefore stays near the ITO/PPV interface. In addition, it was found that the current and the light output of ITO/PPV/Ca PLEDs were reduced more than those of the Au/PPV/Ca PLEDs, a fact that also can be attributed to a reduced hole mobility in the ITO/PPV/Ca devices. We conclude that part of the current and light output reduction of the PLED after heat treatment can be explained by a change of the hole mobility, probably caused by oxygen from the ITO diffusing into the PPV.

4.2. Ca/PPV interface

Electron only single carrier devices, which were heated before calcium deposition, have the same I–V characteristics as devices that were not heated before calcium deposition. This indicates that the PPV itself was not influenced by the annealing step and that reduction of the current was caused by the Ca/PPV interface. From LEIS and XPS experiments it is clear that part of the Ca is diffusing into the PPV during annealing. From XPS it is also clear that during heat treatment no chemical reaction takes place. It is presently not clear what happens if a complete layer of calcium is deposited on the PPV because then the interface cannot be measured with LEIS.

However, LEIS measurements do show that on PPV about 3.5 times as much calcium is needed to form a closed layer as for calcium on silicon. Furthermore the calcium peak in the LEIS spectrum (before heat treatment) is broadened at the low energy side. This can be clearly seen in the

inset in Fig. 6, where LEIS spectra of Ca on PPV and Ca on Si are compared. Both samples had equal surface coverage but the peak of Ca on PPV is much broader. This observation indicates that the Ca/PPV interface is not sharp, because the peak broadening results from He ions, which penetrate the sample and neutralise, subsequently scatter at calcium atoms below the PPV surface, and then re-ionise by the calcium atoms at the surface. From a comparison with the energy loss of He ions in hydrocarbons as reported in [23], it can be estimated that the calcium has diffused up to ~9 nm into the PPV. Note that surface roughness of the PPV does not lead to peak broadening.

It is obvious that a change of the Ca/PPV interface due to annealing will change the injection of electrons into the PPV. Whereas at high fields ($>2.5\times10^3$ V/m) the I–V curves of the electron only devices could be fitted properly by the model used, the currents at low fields could not be reproduced adequately. This can be caused by carrier trapping (e.g. of electrons in the PPV) or calcium diffusion (resulting in an inhomogeneous field distribution at the cathode), which both are not included in this model. As shown in [5,6,24] calcium deposition on PPV leads to new states in the gap by doping the polymer by ionisation of the calcium, which results in quenching sites and charge carrier traps. This can explain the change of the field dependence of the electron mobility. During heat treatment calcium diffuses into PPV and the traps will be present deeper in the PPV and therefore influence the field dependence of the electron mobility.

Another possible cause of the reduction of the field dependence of the mobility of the electrons is an enhancement of structural order in the PPV. However, it can be expected that both the hole and the electron field dependence of the mobility should change due to ordering and furthermore the zero field mobility of the electrons and the holes [21] should increase. This was not observed in our hole and electron only devices. Consequently it is more likely that the change of the field dependence of the mobility at high fields for electron single carrier devices is caused by electron traps or an inhomogeneous electrical field caused by calcium diffusion.

It was shown by Hu and Karasz [11] that a deposition of different cathode materials resulted in different EL spectra. These authors suggested that the first vibronic transition (0–0) is dominated by interface effects. This is in agreement with our observations that the intensity of the first vibronic transition changes after heat treatment, and that heat treatment before calcium deposition does not lead to a change in shape of the electroluminescence spectrum. Devices with an Au/PPV/Ca structure show similar behaviour of the EL spectrum, indicating again that the Ca (or Ca/PPV interface) is the cause of the spectral changes.

Finally, the shift of the maximum of the efficiency curve (Table 1) to higher voltages after annealing, points to an enhanced quenching of excitons at or near the cathode, as shown in [25] where calculations were performed at PLEDs with varying quenching lengths. The calcium that diffused into the PPV is likely to quench the excitons. At higher voltages the area the light was emitted from was located further away from the cathode, where less calcium was present and thus less quenching took place.

5. Conclusions

Heat treatment of PLEDS (ITO/PPV/Ca) leads to a reduction of the current and of the light output. This is caused by the ITO/PPV and the Ca/PPV interfaces. Effects of changes in the PPV itself, if present at all, do not influence the device performance. The degradation of the ITO/PPV interface leads to a decrease of the zero field hole mobility and to an increase of the field dependence of the mobility. This indicates that higher hole barriers are formed in the PPV, probably by diffusion of oxygen from the ITO and subsequent formation of a complex between oxygen and PPV. The degradation of the Ca/PPV interface results in the formation of electron traps and quenching sites. With LEIS and XPS it was shown that calcium diffuses from the Ca/PPV surface into the PPV causing changes of the electron injection and/or transport.

Summarising, we found that heat treatment of ITO/PPV/Ca devices leads, contrary to heat

treatment on ITO/PPV/Al devices [4], to a reduced PLED performance. This is caused by instabilities of the interfaces.

Acknowledgements

The research of F.J.J. Janssen, A.W. Denier van der Gon, L.J. van IJzendoorn, H.F.M. Schoo, M.J.A. de Voigt and H.H. Brongersma is part of the DPI programme. The research of M.K. has been made possible by the Royal Netherlands Academy of Arts and Sciences.

References

[1] J.H. Burroughes, D.D.C. Bradley, A.R. Brown, R.N. Marks, K. Mackey, R.H. Friend, P.L. Burn, A.B. Holmes, Nature 347 (1990) 539.
[2] D. Braun, A.J. Heeger, Appl. Phys. Lett. 58 (1991) 1982.
[3] H.F.M. Schoo, R.J.C.E. Demandt, Philips J. Res. 51 (1998) 527.
[4] T.W. Lee, O.O. Park, Adv. Mater. 12 (2000) 801.
[5] W.R. Salaneck, M. Lögdlund, Polym. Adv. Technol. 9 (1998) 419.
[6] E. Ettedgui, H. Razafitrimo, K.T. Park, Y. Gao, B.R. Hsieh, Surf. Interface Anal. 23 (1995) 89.
[7] L. Bozano, S.A. Carter, J.C. Scott, G.G. Malliaras, P.J. Brock, Appl. Phys. Lett. 74 (1999) 1132.
[8] H.H. Brongersma, H.J. van Daal, Analysis of Microelectronic Materials and Devices, John Wiley & Sons, USA, 1991, Chapter 2.8.
[9] R. Souda, T. Aizawa, C. Oshima, Y. Ishizawa, Nucl. Instr. and Meth. B 45 (1990) 364.
[10] B. Ruhstaller, J.C. Scott, P.J. Brock, U. Scherf, S.A. Carter, Chem. Phys. Lett. 317 (2000) 238.
[11] B. Hu, F.E. Karasz, Chem. Phys. 227 (1998) 263.
[12] E. Peeters, A. Marcos Ramos, S.C.J. Meskers, R.A.J. Janssen, J. Chem. Phys. 112 (21) (2000) 9.
[13] T.Q. Nguyen, V. Doan, B.J. Schwartz, J. Chem. Phys. 110 (1999) 4068.
[14] R. Jakubiak, L.J. Rothberg, W. Wan, B.R. Hsieh, Synth. Met. 101 (1999) 230.
[15] V.N. Bliznyuk, S.A. Carter, J.C. Scott, G. Klärner, R.D. Miller, D.C. Miller, Macromolecules 32 (1999) 361.
[16] P.S. Davids, I.H. Campbell, D.L. Smith, J. Appl. Phys. 82 (1997) 6319.
[17] P.W.M. Blom, M.J.M. de Jong, IEEE J. Sel. Top. Quantum Electron. 4 (1998) 105.
[18] G.G. Andersson, W.J.H. van Gennip, J.W. Niemantsverdriet, H.H. Brongersma, Chem. Phys. 278 (2002) 159–167.
[19] J.C. Scott, J.H. Kaufman, P.J. Brock, R. Dipietro, J. Salem, J.A. Goitia, J. Appl. Phys. 79 (1996) 2745.
[20] F.J.J. Janssen, L.J. van IJzendoorn, H.F.M. Schoo, J.M. Sturm, G.G. Andersson, A.W. Denier van der Gon, H.H. Brongersma, M.J.A. de Voigt, Synth. Met. 131 (2002) 167.
[21] H.C.F. Martens, P.W.M. Blom, H.F.M. Schoo, Phys. Rev. B 61 (2000) 7489.
[22] G.G. Andersson, M.P. de Jong, F.J.J. Janssen, J.M. Sturm, L.J. van IJzendoorn, A.W. Denier van der Gon, M.J.A. de Voigt, H.H. Brongersma, J. Appl. Phys. 90 (2001) 1376.
[23] G. Andersson, H. Morgner, Nucl. Instr. and Meth.: Phys. Res. B 155 (1999) 357.
[24] Y. Park, V.E. Yong, B.R. Hsieh, C.W. Tang, Y. Gao, Phys. Rev. Lett. 78 (1997) 3955.
[25] P.W.M. Blom, M.C.J.M. Vissenberg, J.N. Huiberts, H.C.F. Martens, H.F.M. Schoo, App. Phys. Lett. 77 (2000) 13.